Chemistry in Acetonitrile–Water Films Induced by Slow (

Hassan Abdoul-Carime, Guillaume Thiam, Franck Rabilloud, Florence Charlieux, Janina Kopyra

Chemistry in Acetonitrile-Water Films Induced by Slow (< 15 eV) Electrons: application to the Earth and space chemistry

Hassan Abdoul-Carime[1*], Guillaume Thiam[2], Franck Rabilloud [2], Florence Charlieux [1], Janina Kopyra [3]

[1]Universite de Lyon, Université Lyon 1, Institut de Physique des 2 Infinis, CNRS/IN2P3, UMR5822, F-69003 Lyon, France

[2]Universite de Lyon, Université Claude Bernard Lyon 1, CNRS, Institut Lumière Matière, UMR5306, F-69622 Villeurbanne, France

[3]Faculty of Sciences, Siedlce University of Natural Sciences and Humanities, 3 Maja 54, 08-110 Siedlce, Poland

*Corresponding Author: hcarime@ipnl.in2p3.fr

Keywords: dissociative energy attachment; low-energy electrons; acetonitrile-water films; TD-DFT; methanol; glycolonitrile;

ABSTRACT

Acetonitrile and water are molecules detected not only in space but also in planetary atmospheres. On Earth, the nitrile compound is emitted from the biomass burning and can be found up to the stratosphere. Trapped in water icy cores, they may be exposed to energetic particles, photons and secondary electrons, and contribute to the formation of complex organic molecules. Here, we show that methanol is the main product from the effective reaction of low-energy (<15eV) electrons with acetonitrile-water films deposited on a substrate maintained at 85 K. In this process, each of the molecules is decomposed by the colliding electrons, producing respectively the methyl and the hydroxyl radicals, which further recombine to form methanol, as supported by DFT calculations. In addition, we also report a small production of glycolonitrile, a key precursor of adenine. This information contributes to a better comprehension and description of chemistry on icy grains.

I. INTRODUCTION

Low energy (< 20 eV) electrons have now been shown to be implicated in the chemistry of interstellar medium (e.g., ices [1,2,3]) and planet atmospheres [4,5,6]. They are produced by the primary energetic particles (e.g., galactic cosmic rays, photons) when penetrating in dense media such as icy grains or low atmospheric layers. For instance, the measurements of the low atmospheric structure of Titan (~ 60 km) by the Huygens probe show an abundant production of secondary electrons (c.a., $4.5x10^8$ m^{-3}) [7,8]. Moreover, these ballistic electrons possess a typical energy distribution below 20 eV [9], and they are able to trigger complex chemistry in molecular solids, as it has been demonstrated by the observation of various complex products (e.g., methoxymethanol, ethylene glycol, 1,2,3-propanetriol, …) after the irradiation of films of methanol by 20 eV electrons [10].

Water (H_2O) and acetonitrile (CH_3CN) are compounds detectable in space [11,12,13] and atmospheres [14,15]. The nitriles species are of particular interest. They are not only at the origin of the processes for the formation of prebiotic molecules, but also more specifically acetonitrile is found to be a good tracer of the conditions found in "hot molecular core" phase of massive star formation in warm (> 100K) and dense region [13]. Moreover, CH_3CN is present on icy dusts [16] as well as H_2O and methanol (CH_3OH) and also various other species (e.g., acetone, acetaldehyde, methyl formate) as it has been reported recently [17]. The observations suggest that the complex organic molecules are formed through the surface chemistry triggered by atoms, UV lights, cosmic rays or thermal processing. On Earth, CH_3CN are generated from the biomass burning [18,19] contributing significantly to the local and regional pollutions. The molecule has been found in the atmosphere up to the stratosphere level [20] with a long residence time, ca. 73 years [21], and it can be potentially trapped by water ice cores (e.g., polar stratospheric clouds). Thus, it is desirable to study the chemistry of CH_3CN in presence of H_2O.

The irradiation of pure acetonitrile [22] and pure water [23] ices by high energy particle (> 200 eV) synthetizes predominantly neutral species such as (HC_3N, HCN, …) and (H_2, O_2), respectively. For the acetonitrile-water solids formed at 10 K, the irradiation by 0.8 MeV H^+ ions has been shown to generate complex products such as amino acids [24]. It is noteworthy that in such experiments not only the primary particles but also radicals and the ballistic low energy secondary electrons act all together for the complex chemistry. In a recent study, the irradiation of films composed of an admixture of acetonitrile-water at 20 K with a relatively high density (i.e., > 10^{16} photons cm^{-2}) of 7-12 eV photons resulted in the production of a large variety of species [25]. In this work, we investigate the irradiation of acetonitrile-water (CH_3CN-H_2O) films

by low energy (< 15 eV) electrons at 85 K. We demonstrate that methanol, CH_3OH, is synthesized by typically 10^{13} electrons cm^{-2} and the process involves resonant dissociation of the precursor molecules by the slow particles, followed by radical recombination, as rationalized by DFT calculations. In addition, we report a very weak signal at m/z 56, attributed to glycolonitrile.

II. METHODOLOGIES

Experimental method

The UHV apparatus functioning at a base pressure of 7.10^{-10} mbar is equipped with a trochoidal electron monochromator (TEM), a cryogenically polycrystalline Au substrate (10x8x1) mm^3 mounted on a manipulator, and a commercial quadrupole mass spectrometer (QMS, Balzers) with a home-built extraction system [26]. The TEM based on a dispersive **ExB** fields provides the energy selection ($\Delta E \sim 250$ meV) and also guides the electron beam (of ~ 0.3 cm^2) normally to the substrate. The electron energy is calibrated by a fast record of the electron transmission curve due to the charging of the film during the irradiation [27]. Thus, the incident electron energy is rescaled (every 30 s) until no appreciable shift of the onset of the transmission curve is observed. We estimate the accuracy of the electron energy to be 0.5 eV. The gold substrate is cooled down to 80 K by means of a closed cycle He refrigerator and resistively heated to several hundred Kelvin (> 450 K) for the cleaning. The temperature is measured by a E-type thermocouple fixed to the substrate. Acetonitrile and water (spectroscopic grade), provided from Sigma Aldrich, is purified by repeated freeze-pump-thaw cycles in vacuum before use. The water vapor is introduced to a 27 mL buffer cell before acetonitrile since their respective vapor pressures for preparing an admixture of acetonitrile-water (2:1). This mixed gas is then introduced in the UHV chamber for co-condensing onto the substrate by exposing to a volumetrically calibrated effusing gas quantity (MKS Baratron type 127). In the present experiments, the thickness of the films is evaluated approximately to 5 ML ± 30%, but the exact knowledge of the thickness of the film is not a pre-requisite. Indeed, the films must be thick enough to avoid the effect of the gold substrate, and sufficiently thin to minimize multiple electron inelastic scattering that would modify the electron energy for reaction. For instance, the mean-free path of the electrons in multilayer films has been evaluated to be about 3 nm [28]. For Thermal Programed Desorption Spectrometry, TDS, the species are monitored at a given mass by heating the substrate at a rate of 0.3 K/s (Figures 1 and 2). The desorbed neutral

molecules are detected by recording the positive ions via the electron impact ionization at 70 eV in the QMS and for which the mass spectra of the molecules are well-known [29]. For methanol, the ionization mass spectrum shows the dominant signals (100%) for the $[CH_3OH - H]^+$ (m/z 31) and the $[CH_3OH]^+$ cation (m/z 32) with 100% and ~75% [29]. The m/z 31 signal is usually served as the TDS signature of methanol. However, to avoid potential confusion with species arising from the cracking of glycolonitrile in the mass spectrometer, i.e., m/z 31, 29 and 28 which are common features to methanol, we use the m/z 32 signal. Each data point in Figure 3 is an average value from the irradiation of 2 to 4 fresh films and the estimated reproducibility is 35-40%.

Theoretical method

Calculations were performed in the framework of the density-functional theory (DFT) and the time-dependent DFT (TDDFT) using the range-separated hybrid density functional ωB97x [30]. The resonance electron attachment energies for H_2O are evaluated with a multi-basis-set TDDFT method [31] in which the vertical electron affinity (VEA) is evaluated using DFT calculations with the diffuse basis set aug-cc-pvtz [32] while the anionic excitation energies are calculated using TDDFT and the cc-pvtz basis set [31]. VEA is calculated to be -0.72 eV for H_2O. This relatively low-cost method is well suited for describing valence-type states, but it cannot treat states where the electron lies at long range, e.g. dipole-bound states. Therefore, the resonances of acetonitrile, whose anionic ground state has a dipole-bound characteristic (the electric dipole moment of the molecule is calculated to be 4.07 D, in agreement with the experimental data of 3.924 D [33], while the electron lies by ~10 meV) are obtained with the stabilization method [34] coupled with TDDFT calculations. The excited states of the ion are obtained at ωB97x/aug-cc-pvtz level where the most diffuse exponents of the basis set are scaled by a factor α = 0.2-3, in order to discriminate the discrete continuum states, which correspond to the attachment of the electron, from the continuum states. The energies of the former are expected to be independent of the scaling parameter α, while those of the latter collapse for small values of α.

The anion states presently calculated for acetonitrile and water agree with previous electron transmission spectroscopy [35], DEA[36], R-matrix [37,38] and real-time TDDFT [39] studies. Enthalpies and Gibbs free energies of the fragmentation are calculated at ωB97x/aug-cc-pvtz level at 85 K.

All calculations are performed with the Gaussian16 suite of programs [40]. Pre- and postprocessing operations are performed by using the graphical interface Gabedit [41].

III. RESULTS

Figure 1 presents Temperature Desorption Spectra, TDS, of the pure films served as a references for this work (Figure 2a,b) and TDS from detected species formed from the irradiation of the films by low energy electrons (Figure 2c,d). TDS of water and acetonitrile from co-deposited acetonitrile-water (2:1) films, shown by the red and the blue yields, respectively, in Figure 1a, present maxima at 169 K and 153 K in agreement with already reported studies [42,43, 44]. It is noteworthy that the yield of water (red) is broader than that of the acetonitrile (blue) and the desorption start at the desorption temperature of the nitrile compound. The TDS of pure methanol film shown in Figure 1b (green full-line) also agrees with the literature [43]. The green dashed-yield represents the TDS of methanol from co-deposited methanol-acetonitrile (1:8) film. The shape of the dashed-yield is broader than the green full-line yield, and the temperature is shifted towards that of the desorption temperature of the pure acetonitrile film (Figure 2a, blue yield). This is a clear indication that the desorption of methanol molecules within the film is impeded by the acetonitrile molecules and thus desorb at the temperature of major constituent [45]. Such observation has already been reported for the desorption of methanol from co-deposited water-methanol (20:1): the TDS of the desorbed alcohol matches that of water [44]. A co-deposited acetonitrile-water (2:1) film is then irradiated by an approximately 25 nA beam of 9 eV electrons for 50 minutes. Figure 2c (black line) shows the TDS of methanol observed at its characteristic m/z 32 after the irradiation. The yield is small and the integrated yield represents about 2% of that of the acetonitrile from the freshly deposited acetonitrile-water film. The desorption temperature coincides with that of the acetonitrile, indicating that the synthesized molecules are formed within the film and they desorb along with acetonitrile. An additional specie with very weak intensity is detected at m/z 56. As it will be discussed below, we assign this specie to the glycolonitrile (or hydroxy-acetonitrile), for which the m/z 56 is a characteristic fragment [29]. The TDS of this fragment, also matching that of the acetonitrile (Figure 1d), indicates that this specie is also formed within film, during the irradiation. Otherwise, the presently observed glycolonitrile would be detected to desorb at 225 K [46]. Figure 3 presents the integrated yield of methanol after the irradiation by typically 10^{13} electrons cm^{-2} as the function of the electron energy. The yield function exhibits a threshold at 6 eV and a feature reminiscent of resonant process.

The calculated $[H_2O]^-$ and $[CH_3CN]^-$ anion states are shown in Figures 4 and 5, respectively. The trapping of the extra electron is associated either to a shape resonance (i.e.

accommodation to an empty molecular orbital, e.g., 6.52, 9.10 and 11.66 eV for CH_3CN) or to a core excited resonance (i.e., excitation of one of the molecule valence electron, concomitantly with the trapping of the colliding electron in the Lowest Unoccupied Molecular Orbitals (LUMO)). We have verified that the electronic structure or the resonance energies of the acetonitrile molecule were not affected by the presence of neighboring water molecules in the 5-13 eV range by investigating a cluster of three water molecules surrounding one acetonitrile molecule. Energetics of dissociation reactions are provided in Table 1 and Figure 6. Reactions (a-c) correspond to the fragmentation of the H_2O and the CH_3CN precursor molecules for the production of the $^{\cdot}OH$ and the ($^{\cdot}CH_3$ and $^{\cdot}CH_2CN$) radicals. The associated calculated Gibbs energies indicate the threshold energy required by the colliding electron to trigger the dissociation channels. Radical reactions are represented in schemes (d-h).

IV. DISCUSSION

At the electron energies below 10 eV, the fragmentation of acetonitrile and water molecules arises from Dissociative Electron Attachment (DEA) [36,47,48,49]. This resonant process consists of the capture of the colliding electron into a specific molecular orbital of the target molecule to form a transitory negative ion, $TNI^{\#-}$, (Figure 3a). According to the dynamics (i.e., dissociation time vs. electron autodetachment time) of the metastable anion, the $TNI^{\#-}$ may undergo dissociation producing one negative ion and one or more neutral counterpart(s) [50]. At these energies, the $TNI^{\#-}$ arises from (a) core-excited resonance or (b) shape resonance [52,51]. DEA is experimentally reflected by the peaked structures observed in the detection yield of the fragments [36,47-49]. The yield function presented in Figure 2 exhibits a broad structure indicative of the resonance character for the production of methanol. DEA to water and acetonitrile are now well established and the different dissociation channels and their respective cross-sections are known [36,47-49]. For water, the production of (H^- and $\cdot OH$) is the dominant channel observed from both the gas [36] and the condensed phase studies [49]. The experimentally observed resonance energies agree with the presently calculated states, i.e., excitation of a core electron from the HOMO to LUMO or LUMO+1 concomitantly to the trapping of an electron into the LUMO, which presents a dissociative σ^* character. For the acetonitrile, the gas phase [47] and the film [48] experiments have shown the (CN^- and CH_3) and the (H^- and $\cdot CH_2CN$) channels to be relatively important among all the accessible fragmentation pathways. The temporary anion states are provided in Figure 4 and 5 for water and acetonitrile, respectively. They arise from both the

shape (in grey box) and the core-excited resonances. Commonly to all DEA signals [36,47-49], i.e., CN^-/CH_3CN, H^-/CH_3CN and H^-/H_2O, the threshold of appearance (AE) of the anion signals is observed at around 6-7 eV, and agrees well with the observation of the CH_3OH production (Figure 2).

The synthesized alcohol must arise from the reaction induced by the concomitantly generated radicals, i.e., $\cdot CH_3/CH_3CN$ and the $\cdot OH/H_2O$. Indeed, we have theoretically explored different *scenarios*, listed in Table 1, i.e., reactions (d), (e) and (f). The reactions (e) and (f) for the methanol production, via $\cdot OH + CH_3CN$ and $\cdot CH_3 + H_2O$ are found to be endothermic by 2.37 and 1.10 eV, respectively, indicating that these one-electron processes are not likely to be energetically accessible. In contrast, the reaction between the two close-by radicals, i.e., $\cdot CH_3 + \cdot OH$, initially produced by the decomposition of each precursor by an electron, is found to be exothermic by 3.8 eV (Table 1, reaction (d)), thus energetically accessible. We conclude that the methanol produced in Figure 1c requires (1) DEA to H_2O and, (2) DEA to CH_3CN and (3) recombination of the neighboring methyl and hydroxyl radicals. The broad structure observed in the yield function shown in Figure 3 is reminiscent of the convolution of the yield functions of CN^- (+ CH_3) and H^- (+ OH) reported in Refs. 36,47-49. It is noteworthy that in pure films of water and acetonitrile, radicals reactions $\cdot OH + \cdot OH \rightarrow H_2O_2$ [52] and $\cdot CH_3 + \cdot CH_3 \rightarrow C_2H_6$ [48], respectively, triggered by low energy electrons have been demonstrated. For the pure acetonitrile films, the synthetised C_2H_2 and CH_4 desorb at temperature below 80 K, while HCN has not been directly observed [48,53] but only suggested to be produced [53]. Similarly, for the pure water films, the signal of O_2 has not been shown [52] but, again, suggested to be produced.

The production of glycolonitrile, $HOCH_2CN$, in the present study in spite of the weak intensity of the presently observed signal (Figure 2d), is more exciting in the viewpoint of prebiotic chemistry. Recent reports have suggested this compound to be one of the key species involved in the synthesis of DNA/RNA building blocks [54,55]. Indeed, glycolonitrile, formed via the reaction of HCN with HCHO, may further decompose along with simultaneous oligomerization for adenine. Furthermore, glycolonitrile has also been recently detected in the interstellar medium [56]. From our study, this nitrile-compound can be generated from the reaction of ·OH radical with a close-by CH_3CN molecule or CH_2CN radical, via a one- or two-electron process respectively (Table 1, reaction (g) and (h)). Reaction (h) is found to be endothermic by 0.60 eV while reaction (g) is highly exothermic by 3.37 eV (Table 1), thus most likely accessible in the present experiments. Moreover, the low signal observed m/z 56 signal

suggests that DEA cross section for the decomposition of CH_3CN into (H^- and CH_2CN) must be very low as well.

V. CONCLUSION

The irradiation of acetonitrile:water films (2:1) by low energy electrons presented in these laboratory studies may, in some degrees, reflect a possible rich chemistry in the atmospheric aerosols or space icy dusts. Within the experimental conditions, we show that methanol can also be effectively synthesized by electrons with energies as low as 7 eV. In addition, we are also able to produce, though at a small quantity, a species observed at m/z 56 and assessable to glycolonitrile, a precursor molecule of DNA/RNA building blocks. Moreover, it is noteworthy that the products are detected after the irradiation of typically few 10^{13} electrons cm^{-2} in comparison to UV photolysis experiments (~ 10^{16} photons cm^{-2}) [25].

The present outcomes may, for instance, potentially contribute to a better comprehension of the chemistry occurring of the troposphere of Titan. Indeed, at this altitude (~ 60 km), the temperature meets the high density of the secondary electrons and molecules [57,58], and the formed methanol has been suggested to be a key point for the prediction of the geology [59,60] of the satellite. The information may also increase the knowledge on the chemistry of the Earth's atmosphere. Particularly the poorly understood presence of methanol as the second most abundant atmospheric gas [61] can be related to the emission of CH_3CN from the frequent wildfires burning due to the climate change. Finally, the process in the chemistry of CH_3CN-H_2O triggered by slow electrons might be the initial step to more complex prebiotic molecules [53,62,].

VI. ACKNOWLEDGMENTS

This study was supported by the CNRS MITI–"Défi ORIGINES 2020" (grant number 227617), and the ANR-PRC-BAMBI (grant number 18-CE30-0009-03). In addition, G.T. and F.R. thank the GENCI-IDRIS for supporting the computing time through the grant (A0090807662). JK acknowledges support by the statutory activity subsidy (No 25/20/B) from the Polish Ministry of Science and Higher Education.

VII. TABLES

Table 1: Gibbs free energies of the fragmentation and reactions resulting in the production of methanol or glycolonitrile calculated at ωB97x/aug-cc-pvtz level at 85 K.

Reaction	Gibbs Energy (eV)
DEA	
(a) $H_2O + e^- \rightarrow {}^{\cdot}OH + H^-$	4.17
(b) $CH_3CN + e^- \rightarrow {}^{\cdot}CH_3 + CN^-$	1.31
(c) $CH_3CN + e^- \rightarrow {}^{\cdot}CH_2CN + H^-$	3.23
Production of methanol	
(d) ${}^{\cdot}CH_3 + {}^{\cdot}OH \rightarrow CH_3OH$	-3.80
(e) $CH_3CN + {}^{\cdot}OH \rightarrow CH_3OH + {}^{\cdot}CN$	2.37
(f) ${}^{\cdot}CH_3 + H_2O \rightarrow CH_3OH + {}^{\cdot}H$	1.10
Production of glycolonitrile	
(g) ${}^{\cdot}CH_2CN + {}^{\cdot}OH \rightarrow HO\text{-}CH_2CN$	- 3.37
(h) $CH_3CN + {}^{\cdot}OH \rightarrow HO\text{-}CH_2CN + {}^{\cdot}H$	0.60

VIII. FIGURES

FIGURE 1: Temperature desorption spectra of m/z 32 species (methanol, black), acetonitrile (blue), and water (red). The m/z 32 product is generated from the irradiation of acetonitrile-water (2:1) films for 50 minutes at the electron energy of 9 eV. The acetonitrile and the water spectra are recorded from acetonitrile-water (2:1) films.

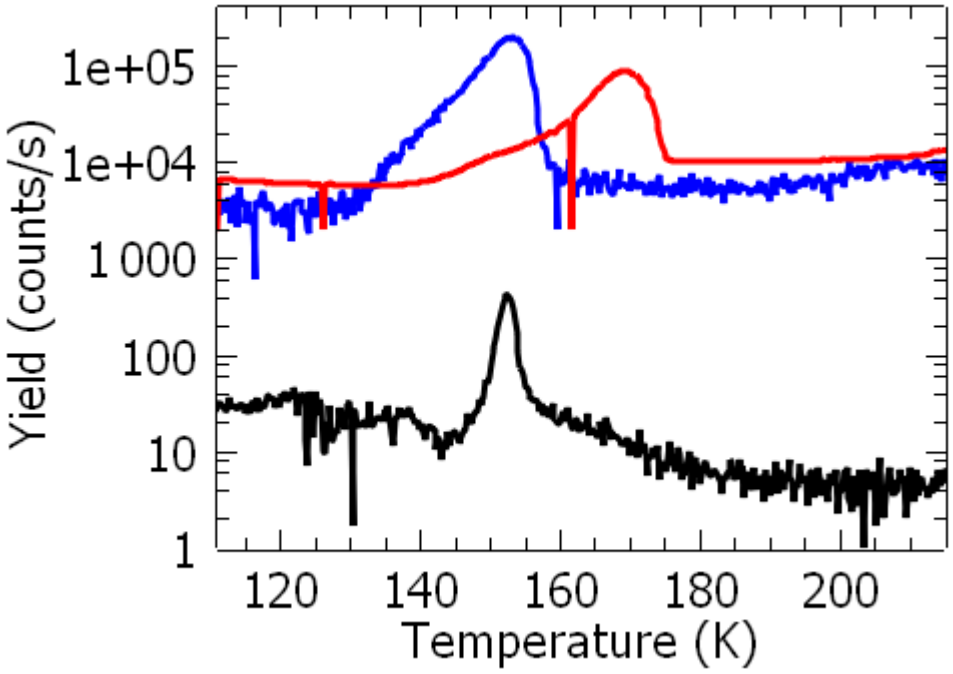

FIGURE 2: Temperature Desorption Spectra from (a) water film (red) and acetonitrile (blue) from a co-deposited acetonitrile-water (2:1) film, (b) pure methanol film (solid green) and methanol from acetonitrile-methanol (8:1) film (dash line), (c) m/z 32 produced after 50 minutes irradiation of acetonitrile-water (2:1) films by 9 eV electrons, (d) m/z 56 after 50 minutes of irradiation of acetonitrile:water (2:1) films by 9 eV electrons.

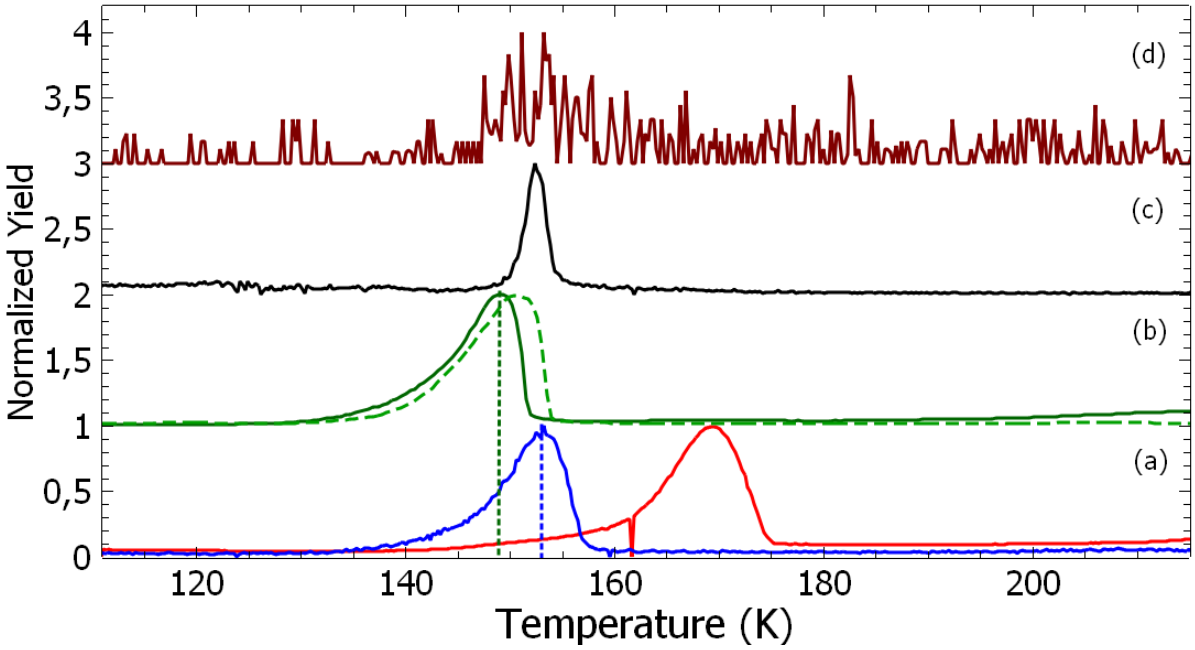

FIGURE 3: Integrated yield of methanol as the function of the incident electron energy. The 35% error bars represent signal reproducibility (film thickness, electron current stability) and the 0.5 eV electron energy accuracy.

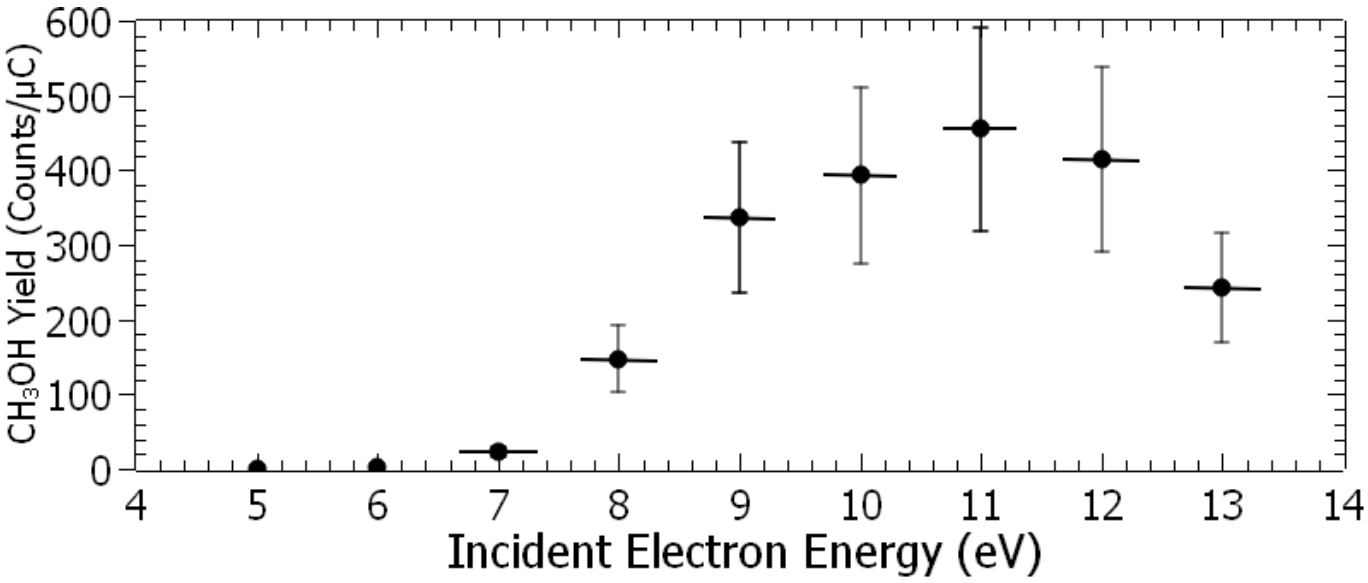

FIGURE 4: Calculated attachment energies (in eV) relative to the neutral ground state of H_2O are given together with the molecular orbitals involved in the trapping of the extra electron. Shape resonances: the orbital occupied by the extra electron is plotted in grey background. Core-excited resonances: trapping of the colliding electron into the LUMO concomitantly with the promotion of a valence electron from the HOMO to the LUMO+n state. Molecular orbitals of the neutral H_2O are provided on the left.

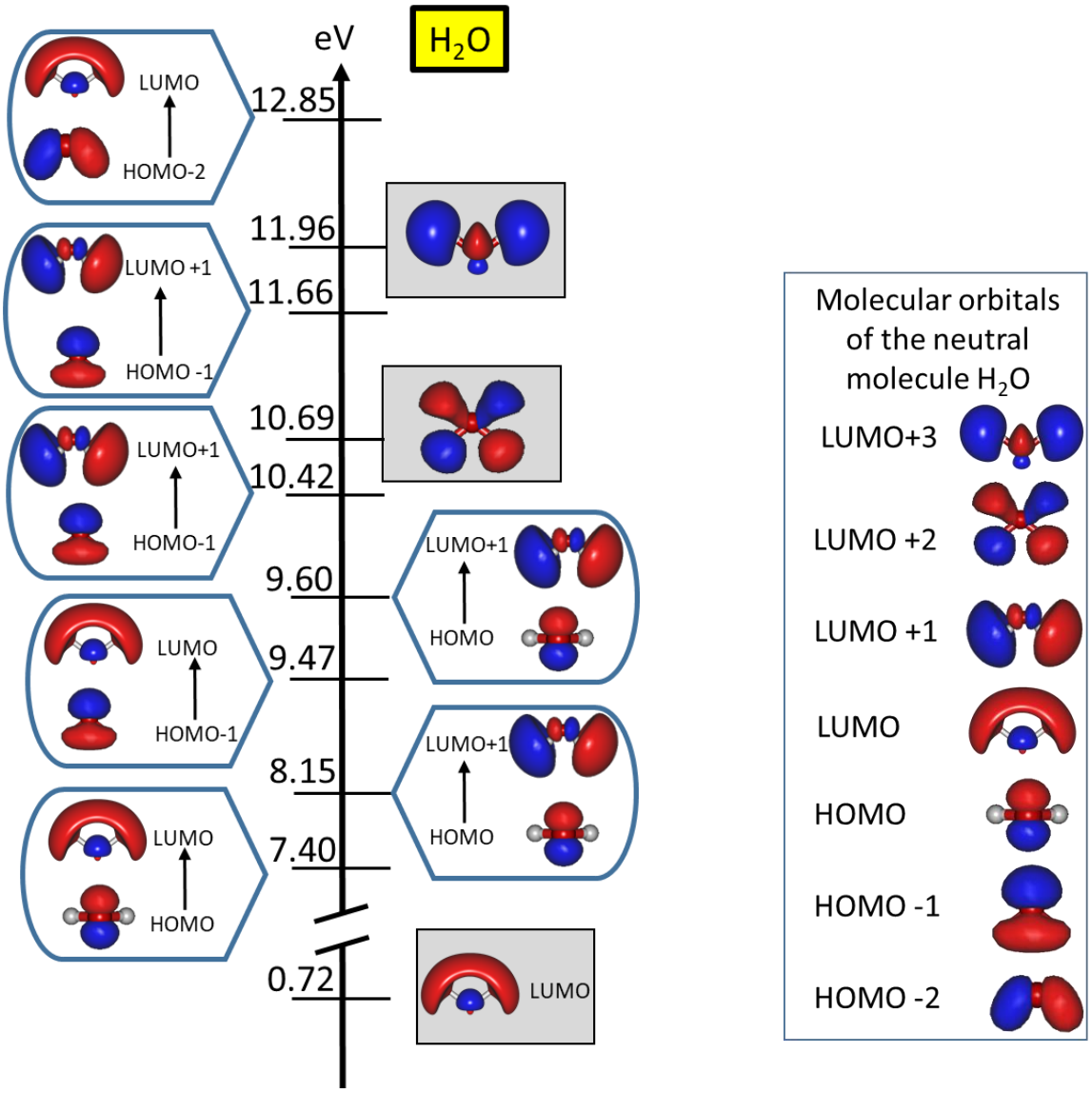

FIGURE 5: Calculated attachment energies (in eV) relative to the neutral ground state of CH_3CN are given together with the molecular orbitals involved in the trapping of the extra electron. Shape resonances: the orbital occupied by the extra electron is plotted in grey background. Core-excited resonances: trapping of the colliding electron into the LUMO concomitantly with the promotion of a valence electron from the HOMO to the LUMO+n state. Molecular orbitals of the neutral CH_3CN are provided on the left.

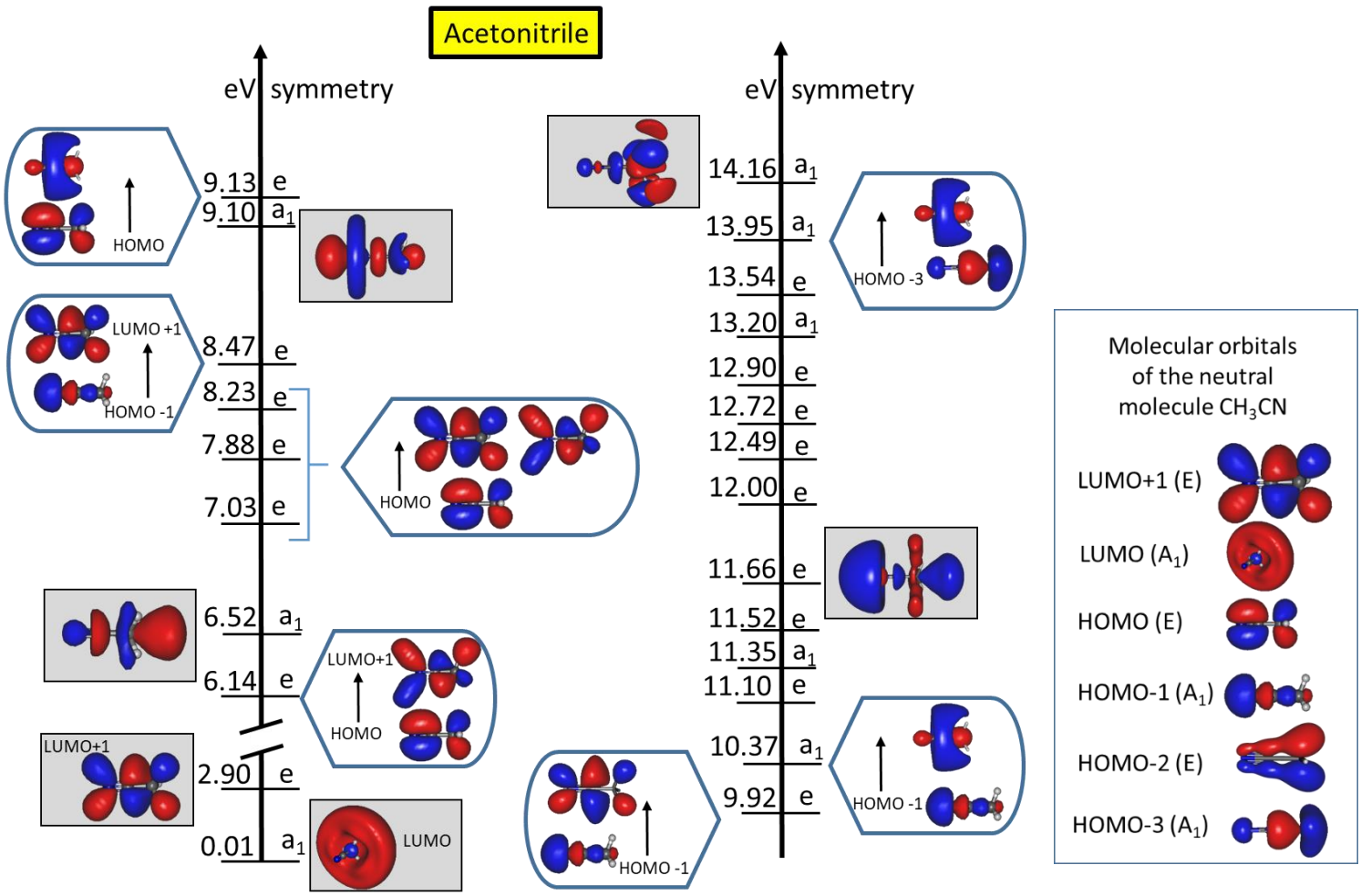

FIGURE 6: Reactions and Gibbs energies for the production of neutral CH_3OH and OH-CH_2CN (Table 1).

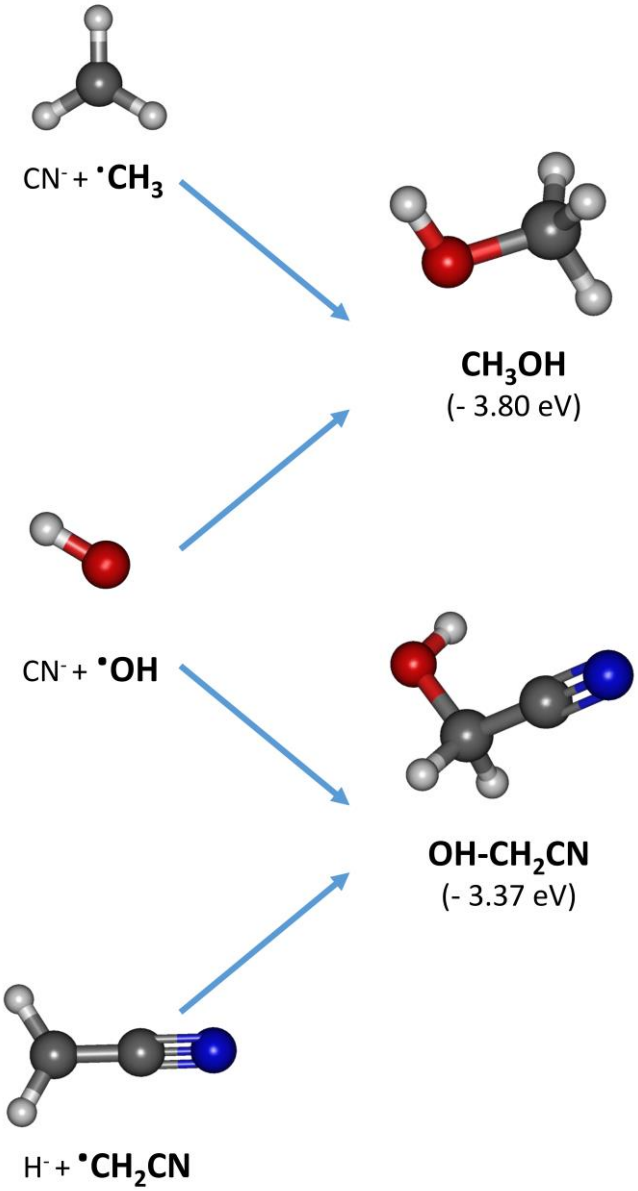

REFERENCES

1 N.J. Mason, B. Nair, S. Jheeta, E. Szymanski, Electron induced chemistry: a new frontier in astrochemistry, *Farad. Discuss.* **168** 235-247 (2014).

2 C.R. Arumainayagam, R.T. Garrod, M.C. Boyer, A.K. Hay, S.T. Bao, J.S. Campbell, J. Wang, C.M. Nowak, M. R. Arumainayagam, P.J. Hodge, Extraterrestrial prebiotic molecules: photochemistry vs. radiation chemistry of interstellar ices, *Chem. Soc Rev.* **48** 2293-2314 (2019).

3 K.E. Shulenberger, J.Zhu, K. Tran, S. Abdullahi, C. Belvin, J. Lukens, Z. Peeler, E. Mullikin, H. Cumberbatch, J. Huang, K. Regovich, A. Zhou L. Heller, et al., Electron-Induced Radiolysis of astronomically relevant ammonia ices, *ACS Earth Space Chem.*, **3** 800-810 (2019).

4 Q.-B. Lu, Cosmic ray driven electron induced reaction of halogenated molecules adsorbed on ice surfaces: implication for atmospheric ozone depletion and global climate change, *Phys. Rep.* 487 141-167 (2010).

5 M.T. Sieger, W.C. Simpson, T.M. Orlando, Production of O_2 on icy satellites by electronic excitation of low temperature ice, *Nature* **394** 554-556 (1998).

6 L. Gan, C.N. Keller, T.E. Craven, Electrons in the ionosphere of Titan, *J. Geophys. Res.* **97** 137-151 (1992).

7 C. Simon-Wedlun, G. Gronoff, J. Lilensten, H. Ménager, M. Bathélemy, Comprehensive calculation of the energy per ion pair or W values for five major planetary atmospheres, *Ann. Geophys.* **29** 187-195 (2001).

8 J.L. Lopez-Moreno, G.J. Molina-Cuberos, H. Hamelin, R. Grard, F. Simões, R. Godard, K. Schweingenschuh, C. Béghin, J.J. Berthelier, V.J.G. Brown, P. Falkner, F. Ferri, M. Fulchignoni, I. Jernej, J.M. Jeronimo, R. Rodrigo, R. Trautner, Structure of Titan's low altitude ionized layer from the Relaxation probe onboard HUYGENS, *Geophys. Res. Lett.* **35** L22104 (2008).

9 M. Mucke, M. Braune, S. Barth, M. Förstel, T. Lischke, V. Ulrich, T. Arion, U. Becker, A. Bradshaw, U. Hergenhahn, A hitherto unrecognized source of low-energy electron in water, *Nature Phys.* **6** 143-146 (2010).

10 Boyer M.C., Rivas N., Tran A.A., Verish C.A., Arumainayagam C.R., The role of low energy (<20 eV) electron in astrochemistry, *Surf. Sci.* **652** 26-32 (2016).

11 H. Calcutt, J.K. Jorgensen, H.S. Müller, L.E. Kristensen, A. Coutens, T.L. Bourke, R.T. Garrod, M.V. Persson, M.H.D. Van der Wiel, E.F. van Dishoek, S.F. Wampfler, The ALMA-PILS survey: complex nitriles towards IRAS 16293-2422 *A&A* **616** A90 (2018).

12 J.B. Bergner, V.G. Guzman, K.I. Oberg, R.A. Loomis, J. Pegues A survey of CH3CN and HC2N in protoplanetary disks, *ApJ* **857** 69 (2018).

13 C.R. Purcell, R. Balasubramanyam, M.G. Burton, A.J. Walsh, V. Minier, M.R. Hunt-Cunningham, L.L. Kedziora-Chudczer, S.N. Longmore, T. Hill, I Brain, P.J. Barnes, A.L.

Busfield, et al. A CH_3CN and HCO^+ survey towards southern methanol maser associated with star formation, *MNRAS* **367** 553-576 (2006).

14 Marten A., Hidayat T., Biraud Y., Moreno R., New millimeter heterodyne observation of Titan: vertical distribution of nitrile HCN, HC_3N, CH_3CN and the isotopic ratio 15N/14N in its atmosphere, *Icarus* **158** 532-544 (2002).

15 Auchettl R., Ruzi M., Appadoo D.R.T., Robertson E.G., Binary phase acetonitrile and water aerosols: infrared studies and theoretical simulation at titan atmosphere conditions, *ACS Earth Space Chem.* **2** 811-820 (2018).

16 E. Herbst, E.F. van Dishoek, Complex organic interstellar molecules, *Ann. Rev. Astronom.* **47** 427-480 (2009).

17 J.E. Lee, S. Lee, G. Baek, Y. Aikawa, L. Cieza, S.-Y. Yoon, G. Harczeg, D. Johnstone, S. Casassus The ice composition in disk around V883 Ori revrealed by its stellar outburst, *Nat. Astronom.* **3** 314-319 (2019).

18 J.A. de Gouw, C. Warneke, D.D. Parrish, J.S. Holloway, M. Trainer, F.C Fehsenfeld, Emission sources and ocean uptake of acetonitrile (CH3CN) in the atmosphere, *J. Geophys. Res: Atmos.* **108** 4329 (2003).

19 Y. Huangfu, B. Yuan, S. Wang, C. Wu, X. he, J. Qi, J. de Gouw, C. Warneke, J.B. Gilma, A. Whisthaler, T. Karl, M. Graus, B.T. Jobson, M. Shao Revisiting acetonitrile as tracer of biomass burning in anthropogenic influenced environments, *Geophys Res. Lett.* **13** 101269 (2021).

20 N.J. Livesey, J.W. Waters, R. Khosravi, G.P. Brasseur, G.S. Tyndall, W.G. Read Stratospheric CH_3CN from the UARS microwave limb sounder, *Geophys Res. Lett.* **28** 799 (2001).

21 J.J. Harrison, P.F. Bernath ACE-FTS observations of acetonitrile in the lower stratosphere, *Atmos. Chem. Phys.* **13** 7405-7413 (2013).

22 A.G.M. Abdulgalil, D. Marchione, J.D. Thrower, M.P. Collings, M.R.S. McCoustra, F. Islam, M.E. Palumbo, E. Congiu, F. Dulieu, Laboratory studies of electron and ion irradiation of solid acetonitrile (CH_3CN), *Phil. Trans. R. Soc. A* **371** 10110586 (2013).

23 A. Galli, A. Vorburger, P. Wurz, A. Pommerol, R. Cerubini, B. Jost ; O. Poch, M. Tulej, N. Thomas, 0.2 to 12 keV electron interacting with water ice: radiolysis, sputtering and sublimation, *Planetary and Space Science* **155** 91-98 (2018).

24 R.L. Hudson, M.H. Moore, J.P. Dworkin, M.P. Martin, Z.D. Pozun, Amino acids from ion-irradiated nitrile-containing ices, *Astrobiol.* **8** 771-779 (2008).

25 M. Bulak, D.M. Paardekooper, G. Fedoseev, H. Linnartz, Photolysis of acetonitrile in a water rich ice as a source of complex organic molecules: CH_3CN and H_2O:CH_3CN ices, *A&A.* **647** A82 (2021).

26 Abdoul-Carime H., Bald I., Illenberger E., Kopyra J., 2018, Selective synthesis of ethylene and/or acetylene from dimethyl sulfide controlled by slow electrons, *J. Phys. Chem. C* **122** 24137-24141.

27 L. Sanche Transmission of 0-15eV monoenergetic electrons through thin-film molecular solids, *J. Chem. Phys.* **71** 4860-4882 (1979).

28 G. Leclerc, T. Goulet, P. Cloutier, J.-P. Jay-Gerin, L. Sanche, Low-energy (0-10 eV) electron transmission spectra of multilayer tryptophan films *J. Phys. Chem.* **91** 4999-5001 (1987).

29 NIST webbook for the Ionization Mass Spectra of hydroxy-acetonitrile or glycolonitrile, methanol, water and acetonitrile

30 J. Chai, M. Head-Gordon Systematic optimization of long-range corrected hybrid density functionals, *J. Chem. Phys*. **128**, 084106 (2008).

31 G. Thiam, F. Rabilloud Multi-Basis-Set (TD-)DFT Methods for Predicting Electron Attachment Energies, *J. Phys. Chem. Lett.* 12 9995-10001 (2021).

32 R.A. Kendall, T.H. Dunning Jr., R.J. Harrison Electron affinities of the first-row atoms revisited. Systematic basis sets and wave functions, *J. Chem. Phys*. **96** 6796-6806 (1992).

33 H. Abdoul-Carime, C. Desfrançois Electrons weakly bound to molecules by dipolar, quadrupolar or polarization forces, *Eur. Phys. J. D* **2**, 149-156 (1998).

34 H.Y. Cheng, Y.S. Huang Temporary anion states of p-benzoquinone: shape and core-excited resonances, *Phys. Chem. Chem. Phys*. **16**, 26306 (2014).

35 A.P. Hitchcock, M. Tronc, A. Modelli Electron transmission and inner-shell electron energy low spectroscopy of acetonitrile, isocyanomethane, methyl thiocyanate and isothiocyanatomethane, *J. Phys. Chem.* **93** 3068-3077 (1989).

36 P. Rawat, V.S. Prabhudesai, G. Aravind, M.A. Rahman M.A. Absolute corss section for dissociative electron attachment to H_2O and D_2O, *J. Phys. B: Atom. Mol. And Optic. Physics*, **40** 4625 (2007).

37 M.M. Fujimoto, E.V.R. de Lima, J. Tennyson Elastic scattering of low energy electrons by CH_3CN and CH_3NC molecules, *Eur. Phys. J. D.* **69** 153 (2015).

38 J.D. Gorfinkiel, L.A. Morgan, J. Tennyson Electron impact dissociative excitation of water within the adiabatic nuclei approximation, *J. Phys. B: At. Mol. Opt. Phys*. **35**, 543-555 (2002).

39 L. Lacombe, P.H.M. Dinh, P.G. Reinhard, E. Suraud, L. Sanche Rare reaction channels in real-time time-dependent density functional theory: the test case of electron attachment, *Eur. Phys. J. D* **140**, 195 (2015).

40 Gaussian 16, Revision C.01, Frisch M.J., Trucks G.W., Schlegel H.B., Scuseria G.E., Robb M.A., Cheeseman J.R., Scalmani G., Barone V., Petersson G.A., Nakatsuji H., Li X., Caricato M., Marenich A.V., Bloino J., Janesko B.G., Gomperts R., Mennucci B., Hratchian H.P., Ortiz J.V., Izmaylov A.F., Sonnenberg J.L., Williams-Young D., Ding F., Lipparini F., Egidi F., Goings J., Peng B., Petrone A., Henderson T., Ranasinghe D., Zakrzewski V.G., Gao J., Rega N., Zheng G., Liang W., Hada M., Ehara M., Toyota K., Fukuda R., Hasegawa J., Ishida M., Nakajima T., Honda Y., Kitao O., Nakai H., Vreven T., Throssell K., Montgomery

Jr. J.A., Peralta J.E., Ogliaro F., Bearpark M.J., Heyd J.J., Brothers E.N., Kudin K.N., Staroverov V.N., Keith T.A., Kobayashi R., Normand J., Raghavachari K., Rendell A.P., Burant J.C., Iyengar S.S., Tomasi J., Cossi M., Millam J.M., Klene M., Adamo C., Cammi R., Ochterski J.W., Martin R.L., Morokuma K., Farkas O., Foresman J.B., Fox D.J., Gaussian, Inc., Wallingford CT, 2016.

41 A.-R. Allouche, A. Gabedi User Interface for Computational Chemistry Softwares, *J. Comput. Chem.* **32**, 174-182 (2011).

42 T. Solomun, K. Christman, H. Baumgärtel Interaction of acetonitrile and benzonitrile with the Au(110) surfaces, *J. Phys. Chem.* **93** 7199-7208 (1989).

43 D.A. Outka, R.J. Madix Brönsted basicity ot atomic oxygen on the Au(110) surface: reaction with methanol, acetylene, water and ethylene, *J. Am. Chem. Soc*. **109** 1708-1714 (1987).

44 M.P. Collings, M.A., Anderson, R. Chen, J.W. Dever, S. Viti, D.A. Williams, D.A. Mc Coustra A laboratory survey of the thermal desorption of astrophysically relevant molecules, *MNRAS* **354** 1133-1140 (2004).

45 R.S. Smith, C. Huang, E.K.L. Wong, B.D. Kay The molecular volcano: Abrupt CCl_4 desorption driven by the crystallization of amorphous solid water, *Phys. Rev. Lett*. **79** 909-912 (1997).

46 A. Fresneau, G. Danger, A. Rimola, F. Duvernay, P. Theulé, T. Chiavassa, Ice chemistry of acetaldehyde reveals competitive reactions in the first step of the Strecker synthesis of alanine: formation of HO-CH(CH_3)-NH_2 vs. HOCH(CH_3)-CN, *MNRAS* **451** 1649-1660 (2015).

47 W. Sailer, A. Pelc, P. Limão-Vieira, N.J. Mason, J. Limtrakul, P. Scheier, M. Probst, T.D. Märk Low energy electron attachment to CH_3CN, *Chem. Phys. Lett.* **381** 216-222 (2003).

48 A.D Bass, J.H. Bredehöft, E. Böhler, L. Sanche, P. Swiderek, Reaction and anion desorption induced by low-energy electron exposure of condensed acetonitrile, *Eur. Phys. J. D.* **66** 53 (2012).

49 X. Pan, H. Abdoul-Carime, P. Cloutier, A.D. Bass, L. Sanche, D^-, O^- and OD^- desorption induced by low energy (0-20 eV) electron impact on amorphous D_2O films, *Radiat. Phys. Chem.* **72** 193 (2005).

50 E. Illenberger, J. Momigny, in *Gaseous molecular ions, An introduction to elementary processes induced by ionization*, Edits H. Baümgartel, E.U. Franck, W. Grünbein, Springer-Verlag Berlin Heidelberg (1992).

51 G. Schulz Resonances in Electron Impact on Diatomic Molecules, *Rev. Mod. Phys*. **45** 423-485 (1973).

52 X. Pan, A.D. Bass, J.-P. Jay-Gerin, L. Sanche A mechanism for the production of hydrogen peroxide and the hydroperoxyle radical on icy satellites by low energy electrons, *Icarus* **172** 521-525 (2004).

53 I. Ipoly, W. Michaelis, P. Swiderek Electron induced reactions in condensed films of acetonitrile and ethane, *PCCP* **9** 180-191 (2007)

54 D.J. Ritson, C. Battilocchio, S.V. Ley, J.D. Sutherland Mimicking the surface and prebiotic chemistry of early Earth using flow chemistry, *Nat. Comm.* **9** 1821 (2018).

55 M.E. Schrader, The RNA world: conditions for prebiotic synthesis, *J. Geophys. Res.* **114** D15305 (2009).

56 S. Zeng, D. Quénard, I. Jiménez-Serra, J. Martin-Pintado, V.M. Rivilla, L. Testi, R. Martin-Domenech, First detection of the prebiotic molecule glycolonitrile ($HOCH_2CN$) in the interstellar medium, *MNRAS* **484** L43-48 (2019).

57 B. Kazeminejad, H. Lammer, A. Coustenis, O. Witasse, G. Fischer, K. Schweingenschuh, A.J. Ball, H.O. Rucker H.O., 2005, Temperature variation in Titan's upper atmosphere: Impact on Cassini/Huyghens, *Annales Geophysicae* **23** 1183-1189 (2005).

58 J.L. Lopez-Moreno, G.J., Molina-Cuberos, H. Hamelin, R. Grard, F. Simões, R. Godard, K. Schweingenschuh, C. Béghin, J.J. Berthelier, V.J.G. Brown, P. Falkner, F. Ferri, M. Fulchignoni, I. Jernej, J.M. Jeronimo, R. Rodrigo, R. Trautner, Structure of Titan's low altitude ionized layer from the Relaxation probe onboard HUYGENS, *Geophys. Res. Lett.* **35** L22104 (2008).

59 M. Neveu, S.J. Desch, J.C. Castillo-Rogez Aqueous geochemistry in icy world interior: Equilibrium fluid, rock and gas compositions and fate of antifreezes and radionucleides, *Geochemica et Cosmochimica Acta* **212** 324371 (2017).

60 Deschamps F., Mousis O., Sanchez-Valle C., Lunine J.I. The role of methanol in the crystallization of Titan's primordial ocean, *Astrophys. J.* **724** 887-894 (2010).

61 K.H. Bates, D.J. Jacobs, S. Wang, R.S. Hornbrook, E.C. Apel, M.J. Kim, D.B. Millet, K.C. Weels, X. Chen, J.F. Brewer, E.A. Ray, R. Commane et al., The global budget of atmospheric methanol: new constrains on secondary oceanic and terrestrial sources, J.G.R. *Atmospheres* 129 e2020JD033439 (2021).

62 S.M. Hörst, R.V. Yelle, A. Buch, N. Carrasco, G. Cernogora, O. Dutuit, E. Quirico, E. Sciamma-O'Brien, M.A. Smith, A. Somogyi, C. Szopa, R. Thissen, V. Vuitton Formation of Amino-Acids and nucleotide bases in a Titan Atmosphere Simmulation Experiment, *Astrobiol.* **12** 809-817 (2012).

Graphical Table of Content

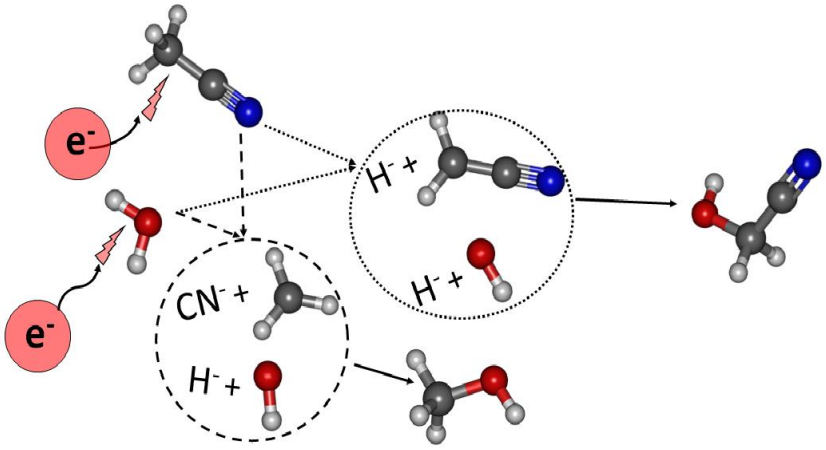

Chemistry in Acetonitrile-Water Films Induced by Slow (< 15 eV) Electrons: application to the Earth and space chemistry

by

Hassan Abdoul-Carime [1], Franck Rabilloud [2], Guillaume Thiam [2], Florence Charlieux [1], Janina Kopyra [3]

[1]*Universite de Lyon, Universite Lyon 1, Institut de Physique des 2 Infinis, CNRS/IN2P3, UMR5822, F-69003 Lyon, France*

[2]*Universite de Lyon, Universite Claude Bernard Lyon 1, CNRS, Institut Lumiere Matiere, UMR5306, F-69622 Villeurbanne, France*

[3]*Faculty of Sciences, Siedlce University of Natural Sciences and Humanities, 3 Maja 54, 08-110 Siedlce, Poland*

Supplementary

Figure S1: Temperature desorption spectra of the (a) m/56 amu and, (b) m/z 32 species. They are recorded after 50 min of irradiation of acetonitrile-water (2:1) films by a 9 eV electron beam. The dashed line are obtained from “blanc” experiments for unirradiated films.

(a)

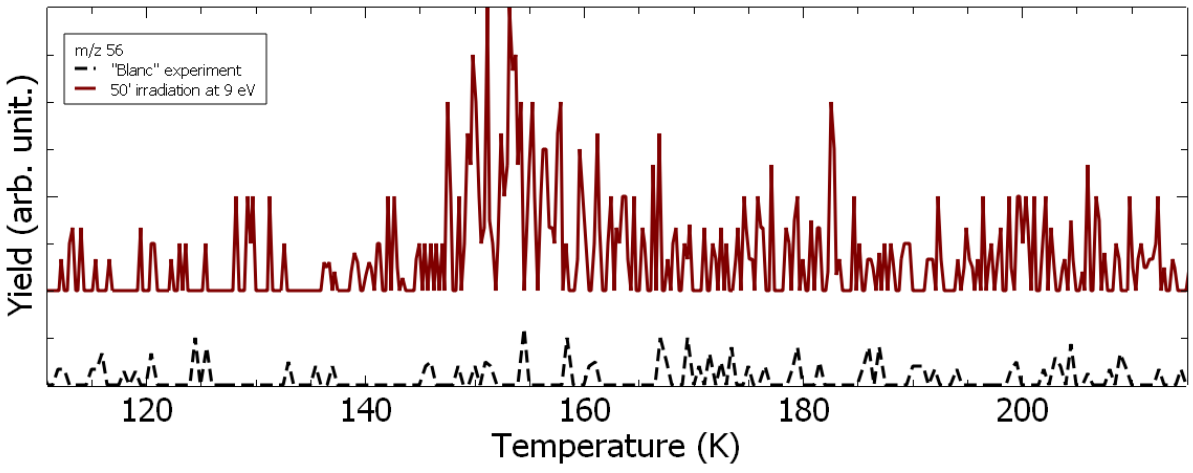

(b)

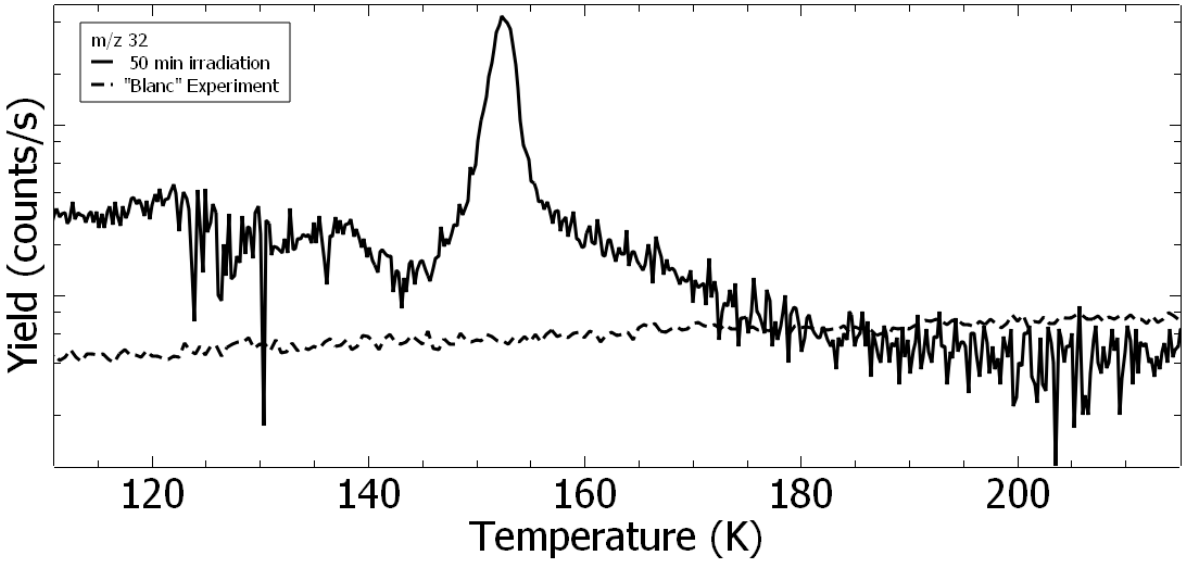

Figure S2: Geometry obtained for a cluster containing 3 water molecules and 1 molecule of acetonitrile. Geometry optimization done at the ωB97xD/aug-cc-pvtz level.

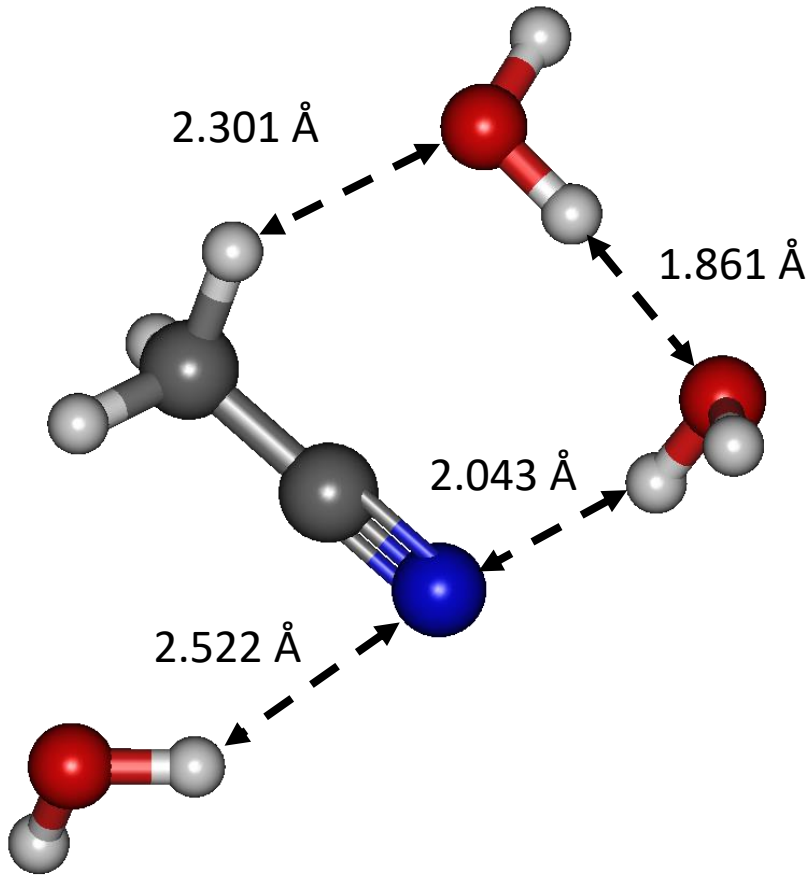

Figure S3: Calculated attachment energies (in eV) for the acetonitrile molecule surrounded by three water molecules. The energies relative to core-excited states (6.29, 7.10 and 8.20 eV) are very close to those of obtained in gas phase (6.14, 7.03 - 8.23 eV, see figure 5). The shape resonance energies are shifted to lower values compared to the gas phase (Figure 5): the shape resonance calculated at 2.90 eV in gas phase is shifted to 2.52 eV, that obtained at 6.52 eV is now between 6.55 and 6.82 eV, that at 9.10 eV is between 7.97 and 8.63 eV.

Due to the size of the basis set and the number of atoms, the number of excited states is highly increased, and it becomes quite difficult to have quantitative results above 9 eV excitations hence we preferred focusing on states with energies between 6 eV and 9 eV.

*Two values are given, due to the presence of an avoided crossing. Such states would require the use of the stabilization method to obtain the value from a plateau (G. Thiam, F.Rabilloud, J. Phys. Chem. lett. 12, 9995 (2021))). Here, with a single point calculation, we just furnish lower and upper limits.